Universiteit Leiden
The Netherlands

Identification of glucose kinase dependent and independent pathways for carbon control of primary metabolism, development and antibiotic production in Streptomyces coelicolor by quantitative proteomics

Gubbens, J.; Janus, M.; Florea, B.I.; Overkleeft, H.S.; Wezel, G.P. van

Citation
Gubbens, J., Janus, M., Florea, B. I., Overkleeft, H. S., & Wezel, G. P. van. (2012). Identification of glucose kinase dependent and independent pathways for carbon control of primary metabolism, development and antibiotic production in Streptomyces coelicolor by quantitative proteomics. *Molecular Microbiology*, *86*(6), 1490-1507. doi:10.1111/mmi.12072

Version: Publisher's Version
License: Licensed under Article 25fa Copyright Act/Law (Amendment Taverne)
Downloaded from: https://hdl.handle.net/1887/3203972

Note: To cite this publication please use the final published version (if applicable).

Molecular Microbiology (2012) 86(6), 1490–1507 ■
doi:10.1111/mmi.12072
First published online 5 November 2012

Identification of glucose kinase-dependent and -independent pathways for carbon control of primary metabolism, development and antibiotic production in *Streptomyces coelicolor* by quantitative proteomics

Jacob Gubbens, Marleen Janus, Bogdan I. Florea, Herman S. Overkleeft and Gilles P. van Wezel*
Leiden Institute of Chemistry, Leiden University, PO Box 9502, 2300RA, Leiden, The Netherlands.

Summary

Members of the soil-dwelling prokaryotic genus *Streptomyces* are indispensable for the recycling of complex polysaccharides, and produce a wide range of natural products. Nutrient availability is a major determinant for the switch to development and antibiotic production in streptomycetes. Carbon catabolite repression (CCR), a main signalling pathway underlying this phenomenon, was so far considered fully dependent on the glycolytic enzyme glucose kinase (Glk). Here we provide evidence of a novel Glk-independent pathway in *Streptomyces coelicolor*, using advanced proteomics that allowed the comparison of the expression of some 2000 proteins, including virtually all enzymes for central metabolism. While CCR and inducer exclusion of enzymes for primary and secondary metabolism and precursor supply for natural products is mostly mediated via Glk, enzymes for the urea cycle, as well as for biosynthesis of the γ-butyrolactone Scb1 and the responsive cryptic polyketide Cpk are subject to Glk-independent CCR. Deletion of *glkA* led to strong downregulation of biosynthetic proteins for prodigionins and calcium-dependent antibiotic (CDA) in mannitol-grown cultures. Repression of *bldB*, *bldN*, and its target *bldM* may explain the poor development of *S. coelicolor* on solid-grown cultures containing glucose. A new model for carbon catabolite repression in streptomycetes is presented.

Accepted 14 October, 2012. *For correspondence. E-mail g.wezel@chem.leidenuniv.nl; Tel. (+31) 71527430; Fax (+31) 715274340.

© 2012 Blackwell Publishing Ltd

Introduction

The ability to sense and select the carbon sources that allow fastest growth is the driving force for the evolution of carbon regulation in bacteria, and offers selective advantage because it optimizes the chance of survival. The underlying control process of carbon catabolite repression (CCR) ensures that when a primary carbon source such as glucose is available, the utilization of secondary carbon sources is repressed, even if these carbon sources are present in significant quantities (Brückner and Titgemeyer, 2002; Gorke and Stulke, 2008).

Streptomycetes are Gram-positive, soil-dwelling, multicellular bacteria that undergo complex morphological development. They produce a wide range of secondary metabolites, including antibiotics and anti-cancer compounds, with approximately two-thirds of the known natural antibiotics synthesized by actinomycetes (Demain, 1999; Hopwood, 2007). Soils and aquatic sediments fluctuate in the availability of nutrients, and the saprophytic streptomycetes produce various extracellular enzymes such as chitinases, amylases, proteases and cellulases, which allow them to feed on most if not all naturally occurring polymers (Chater *et al.*, 2010). Initially, streptomycetes form a network of branched hyphae, the vegetative mycelium, and once the checkpoint for the initiation of differentiation has been passed, a dedicated aerial mycelium is produced, using the vegetative mycelium as a substrate (Chater, 2001). The aerial hyphae then undergo several morphological stages before committing themselves to sporulation (Flärdh and Buttner, 2009), following an unusually complex process of co-ordinated multiple cell division and DNA segregation (Jakimowicz and van Wezel, 2012). Proteins that control the onset of aerial hyphae formation are called Bld ('bald', so-called as they fail to produce the fluffy aerial hyphae), and those that control sporulation are called Whi ('white', for their failure to produce grey-pigmented spores). Development and antibiotic production of streptomycetes are likely subject to CCR, which is best illustrated by the fact that many *bld* mutants are only blocked in development in the presence

of glucose and other repressing carbon sources (Ingram and Westpheling, 1995; Pope *et al*., 1996; recently reviewed in Sanchez *et al*., 2010; van Wezel and McDowall, 2011).

Carbon source utilization in bacteria is mediated through three different types of import systems: the phosphoenolpyruvate-dependent phosphotransferase system (PTS; Brückner and Titgemeyer, 2002), the ATP-binding cassette transporters (ABC-transporters; Davidson *et al*., 2008) and proteins of the major facilitator superfamily (MFS; Pao *et al*., 1998). During PTS-mediated carbon source internalization, a phosphoryl group is transferred from the glycolytic intermediate phosphoenolpyruvate, via the PTS enzymes phosphotransferase enzyme I (EI), the histidine phosphor-carrier protein (HPr), and Enzyme IIA (EIIA) onto the incoming carbon source. In most bacteria, the PTS plays a major role in CCR, with PTS-mediated transport triggering the cAMP-receptor protein (Crp) in Gram-negative bacteria, and the catabolite control protein CcpA in low-GC Gram-positive bacteria (Brückner and Titgemeyer, 2002). In *Streptomyces*, glucose transport is not mediated via the PTS, but via the MFS transporter GlcP (van Wezel *et al*., 2005), and in terms of global regulation streptomycetes lack a CcpA orthologue, while Crp is present but does not play a role in CCR (Piette *et al*., 2005). Therefore, an alternative control mechanism must be in place for CCR.

In streptomycetes the enzyme glucose kinase (Glk; SCO2126) not only converts glucose to glucose-6P, but also plays a central role in carbon catabolite repression, and deletion of *glkA* gene results in global loss of CCR (Angell *et al*., 1992; Kwakman and Postma, 1994). Interestingly, CCR is independent of the Glk enzymatic activity and the flux of glucose, and replacing Glk of *Streptomyces coelicolor* by that of *Zymomonas mobilis* restores normal glycolysis, but not CCR (Angell *et al*., 1994). However, attempts to separate these two activities in Glk itself via directed mutagenesis have failed so far (van Wezel and McDowall, 2011). SCO2127, which is located directly upstream of *glkA*, stimulates the transcription of *glkA* and restores CCR in mutants of *S. peucetius* var. *caesius* that are resistant to the inhibition of carbon source utilization by 2-deoxyglucose (Guzman *et al*., 2005). Glk of *S. coelicolor* belongs to group III of the glucose kinases, found primarily in Gram-positive bacteria and archaea (Lunin *et al*., 2004). The group III family glucose kinases contain a ROK signature found in a diverse family of proteins (repressors, ORFs & kinases; Titgemeyer *et al*., 1994). Recently, the structure of Glk of *Streptomyces griseus* was solved (Miyazono *et al*., 2012). In contrast to many ROK-family proteins Glk does not contain a DNA-binding motif. Instead, the mode of action involves binding of Glk to the GlcP transporter, and Glk is perhaps released from GlcP during the transport of glucose (van Wezel *et al*., 2007). Glk is produced constitutively in liquid cultures of *S. coelicolor* (Mahr *et al*., 2000), but the enzymatic activity depends on the growth phase and carbon source, with much higher enzymatic activity in glucose-grown cultures than in mannitol (van Wezel *et al*., 2007).

In this work we provide a detailed quantitative proteomics analysis of *S. coelicolor* and its *glkA* deletion mutant. This allowed us to detail the metabolic targets of Glk-dependent and Glk-independent carbon control via advanced proteomics, with quantification of the expression levels of some 25% of the *S. coelicolor* proteome depending on the carbon source, including virtually all enzymes for central metabolism and enzymes for the antibiotic biosynthetic machineries. This established the presence of Glk-dependent and Glk-independent CCR control of central metabolism and antibiotic production.

Results

To obtain insight into the effect of glucose on global protein expression in *Streptomyces*, and into the role of Glk (SCO2126) in both glycolysis and CCR, we compared the global protein expression profiles of the *S. coelicolor glkA* mutant and its parent M145 in liquid-grown NMMP cultures at mid-exponential growth phase with different combinations of carbon sources (Fig. 1). First, mannitol was used as a reference non-repressing carbon source and compared with growth in the presence of additional glucose for both strains. Stable isotope dimethyl labelling of peptides (Boersema *et al*., 2009) was used to perform a quantitative proteomics comparison as this method is not dependent on labelling of growth media. However, since only three samples could be compared simultaneously, the four samples were split in two mixtures (Fig. 1A). After LC-MS/MS analysis the data from these two mixtures were again combined in one analysis run to yield four comparisons that differed only in carbon source or in the presence or absence of *glkA* (Fig. 1B, solid arrows). One comparison (Fig. 1B, dashed arrows) could be measured in both mixtures and was therefore considered a technical replicate (Fig. 1C). To analyse the role of Glk during active flux through glycolysis, an identical experiment was performed substituting mannitol with fructose (Fig. 1A, B, and D).

For both experiments a linear fit could be obtained for the technical replicate between the two mixtures (Fig. 1C and D), although the correlation was less for the experiment using mannitol as comparative carbon source. Possibly, this is due to lower number of data points (399 vs 1053 using fructose) resulting in less quantifications demonstrating a large difference in expression (^{2}log ratio < -1 or > 1). As a control for biological relevance, Pearson correlations were also calculated to compare the experiment using mannitol as comparative carbon source with the experiment using fructose (Table S1). Each comparison in

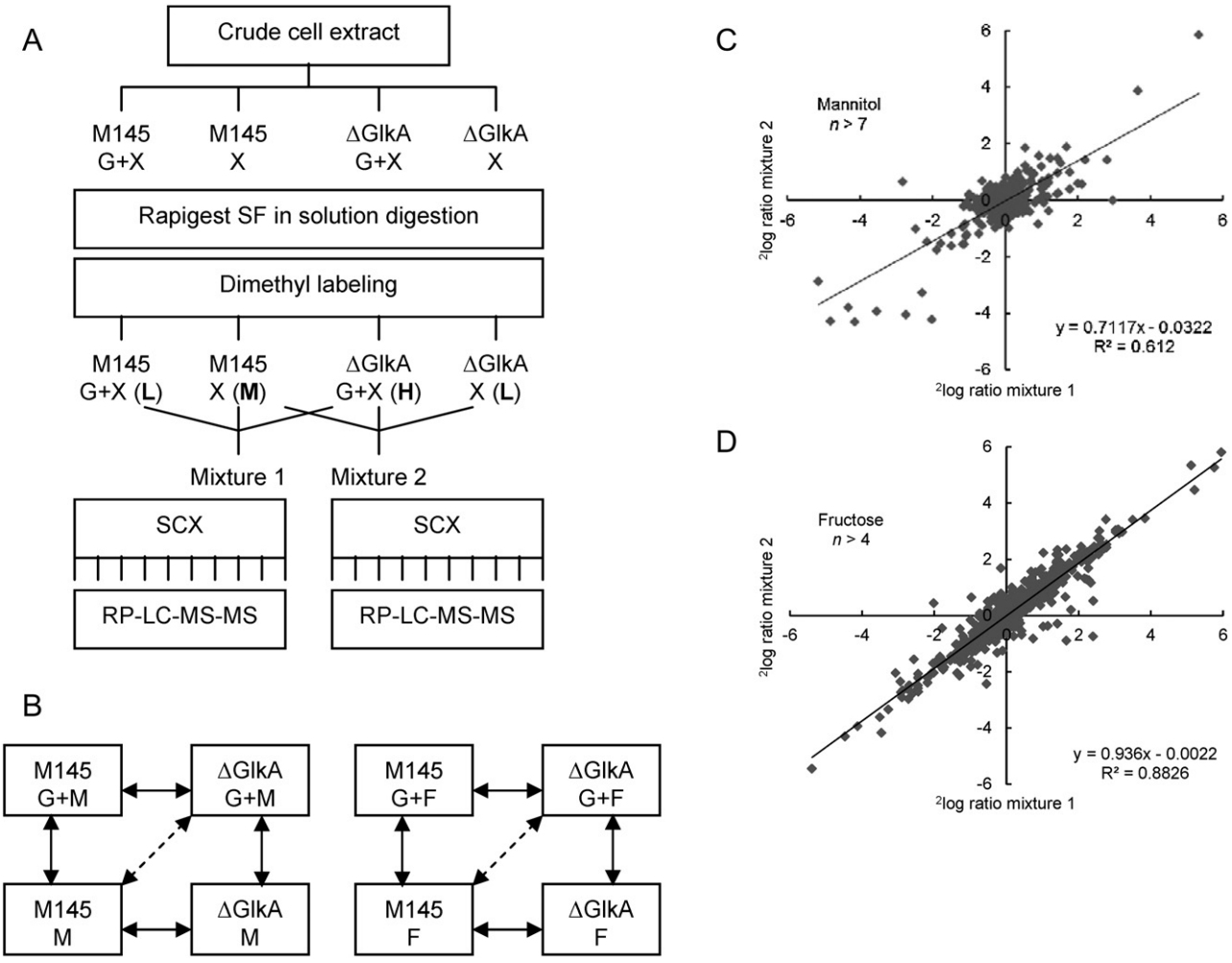

Fig. 1. Overview of the mass spectrometry-based quantitative proteomics strategy.
A. The dimethyl labelling method used for multiplexed comparative analysis of proteins from *S. coelicolor* M145 and its *glkA* mutant derivative grown on different carbon sources. G stands for glucose, X is the comparative carbon source, namely mannitol in the first proteomics experiment, and fructose in the second experiment. L, M, H indicates light, medium, or heavy stable isotope labelling respectively. Since dimethyl labelling allows for the comparison of three samples while the experiments contained four samples, two mixtures were prepared for each experiment and analysed by LC-MS/MS.
B. After data analysis, four comparisons per experiment were obtained that differed only in carbon source or *glkA* deletion (solid arrows). One comparison was obtained for both mixtures in each experiment (dashed arrows) as a technical replicate.
C and D. These replicates were correlated to judge reproducibility between the mixtures for the experiment with mannitol (C), and fructose (D) as comparative carbon source.

the mannitol background was best correlated to the identical experiment in the fructose background ($0.25 < r < 0.5$), with one exception: The Δ*glkA*/M145 comparison in fructose was more similar to the same comparison in glucose plus mannitol than in mannitol only (0.403 vs 0.249). Clearly, this can be explained by a preference of fructose/glucose as carbon source over mannitol.

In total more than 2350 proteins could be positively identified of which 1937 were quantified in at least three MS events for one of the comparisons, representing over 25% of the putative *S. coelicolor* proteome (Table S2). Therefore, this approach, aimed at the comparison of protein expression profiles in multiple varying conditions, improved the dynamic range described in previous iTRAQ labelling proteomics experiments that allowed comparison of some 8–9% of the *S. coelicolor* proteome (Manteca *et al.*, 2010a,b) with high reproducibility.

Central metabolism

Glycolysis to the TCA cycle. The flux of glucose in *S. coelicolor* and the enzymes involved are highlighted in Fig. 2. All glycolytic enzymes were detected and in most cases expression was induced by glucose (Table 1). The upregulation in *glkA* mutant cells strongly suggests that *glkA* is not required for glycolytic signalling, but rather that this is

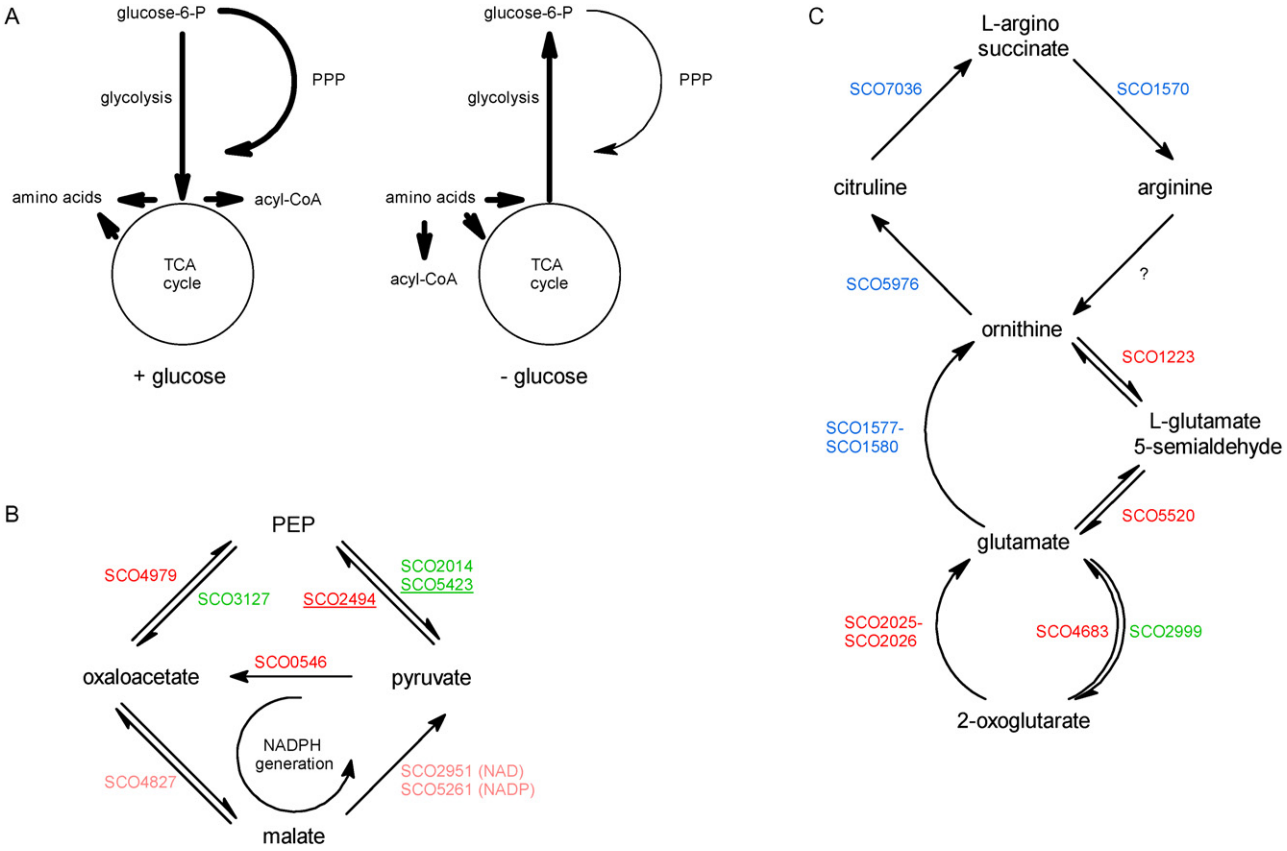

Fig. 2. Changes in central metabolism in response to glucose availability and *glkA* deletion.
A. General overview of central metabolism in the presence or absence of glucose as measured by changes in protein expression levels. When glucose is available, utilization of other carbon sources is excluded. However, when glucose is not available, amino acids are used as carbon source, providing acyl-CoA for fatty acid and polyketide synthesis. PPP is the pentose phosphate pathway.
B. Overview of the anaplerotic node in *S. coelicolor*. Enzymes subject to CCR (glucose repression) are shown in red, those activated by glucose in green. In case glucose repression/stimulation was not lost in the *glkA* deletion mutant (i.e. is Glk-independent), the enzyme is underlined. An alternative pathway to generate NADPH in the absence of glucose (independent of PPP) is indicated.
C. Overview of glutamate metabolism and the urea cycle. Proteins indicated in red are subject to Glk-dependent CCR. Proteins indicated in blue demonstrate a typical expression pattern for urea cycle proteins of Glk-independent CCR when grown on fructose.

mediated via the glucose transporter GlcP. Accumulation of GlcP itself (encoded by the identical genes SCO5578 and SCO7153; van Wezel *et al*., 2005) was strongly enhanced by glucose in a Glk-independent manner, with massive upregulation (some 16-fold) in the *glkA* mutant. We also identified nearly all enzymes of the TCA (tricarboxylic acid) cycle, whose expression was largely unchanged (Table S3).

The three isoforms for the glycolytic enzyme glyceraldehyde-3-phosphate dehydrogenase (SCO1947, SCO7040 and SCO7511) showed significant divergence in their expression. While Gap1 (SCO1947) showed similar induction by glucose as the other glycolytic enzymes, Gap3 (SCO7511) was also induced by glucose, but only in the presence of *glkA*, while Gap2 (SCO7040) was glucose repressed, with a pattern conforming to that of enzymes of the gluconeogenesis pathway (see below), suggesting that Gap2 might antagonize Gap1/Gap3. Expression of both pyruvate kinase isoforms Pyk1 (SCO2014) and Pyk2 (SCO5423) was induced by glucose, but while this occurred in a Glk-dependent manner for Pyk1, it was independent of Glk for Pyk2.

The anaplerotic node and gluconeogenesis. Gluconeogenesis effects the opposite of glycolysis, producing glucose from non-carbohydrate substrates and starts at the anaplerotic node that links the TCA cycle and glycolysis/gluconeogenesis (Sauer and Eikmanns, 2005) (Fig. 2B). Expression of the gluconeogenic PEP carboxykinase (PEPCK; SCO4979), which catalyses the conversion from oxaloacetate to phosphoenolpyruvate (PEP), is 8–30-fold repressed by glucose (Table 1). In contrast, the enzyme PEP carboxylase (SCO3127) that catalyses the reverse anaplerotic reaction (production of oxaloacetate from PEP), showed the exact mirror response. Fructose-1,6-bisphospatase (GlpX; SCO5047), the rate limiting

Table 1. Carbon-source-dependent expression profiles of enzymes involved in central sugar metabolism.

Strain[a]	Δ*glkA*/M145	Δ*glkA*/M145	Δ*glkA*	M145	Δ*glkA*/M145	Δ*glkA*/M145	Δ*glkA*	M145	
Condition	M	GM	GM/M	GM/M	F	GF	GF/F	GF/F	Known or predicted function
Glycolysis									
SCO5578/SCO7153[b]					0.9[c]	1.5	4.1	5.0	GlcP, glucose transporter
SCO1942	−0.9	−0.8	1.6	1.3	−0.6	−0.1	0.0	−0.7	Pgi2 Glucose 6-phosphate isomerase 2
SCO6659	−1.5	−0.4	3.3	2.5	0.3	0.3	1.9	1.6	Pgi Glucose 6-phosphate isomerase 1
SCO1214		−2.2		1.4					PfkA3 pfk3 6-phosphofructokinase 3
SCO5426		−0.4		0.3	−0.3	1.7	2.4	−0.3	PfkA2 pfk2 6-phosphofructokinase 2
SCO3649	−0.6	−0.7	0.1	0.7	−0.2	0.4	0.8	0.3	Fba Fructose-bisphosphate aldolase
SCO1945	−0.1	−0.3	0.1	0.5	−0.1	0.2	0.7	0.4	Tpi Triosephosphate isomerase
SCO1947	−1.8	−0.7	2.6	1.6	0.3	−0.5	1.7	2.6	Gap1 Glyceraldehyde-3-phosphate dehydrogenase
SCO7040	0.5	4.7	0.5	−2.4	0.2	5.3	0.8	−4.1	Gap2 Glyceraldehyde-3-phosphate dehydrogenase
SCO7511	−0.3	−2.0	−0.8	2.6	0.8	−2.2	−0.7	2.7	Gap3 Glyceraldehyde 3-phosphate dehydrogenase
SCO1946	−1.0	−0.2	1.3	0.5	0.1	−0.3	0.6	0.8	Pgk Phosphoglycerate kinase
SCO2576	0.4		−0.9		−0.2	−0.2	0.0	0.2	Pgm2 Phosphoglycerate mutase
SCO4209	−2.0	−0.6	1.5	0.5	−0.3	−0.7	0.2	−0.8	GpmA gpm pgm phosphoglycerate mutase
SCO3096	0.2	1.3	1.6	0.4	0.3	1.2	1.3	0.2	Eno1 Enolase 1
SCO7638		−2.6		−0.9					Eno2 Enolase 2
Anaplerotic node & gluconeogenesis									
SCO2014	−0.5	−1.1	0.2	0.2	−0.6	−1.5	−0.5	1.1	Pyk1 Pyruvate kinase
SCO5423	−0.5	−0.6	2.2	1.7	0.6	−0.3	1.7	2.4	Pyk2 Pyruvate kinase
SCO3127	−1.7	−2.3	0.4	1.1	0.3	−1.0	0.7	1.9	Ppc Phosphoenolpyruvate carboxylase (PEPC)
SCO0546	1.9		−1.0		0.4	1.2	0.1	−0.9	Pyc Pyruvate carboxylase
SCO2951	−0.1	0.6	−0.2	−0.4	−0.3	0.2	−0.2	−0.8	Putative malate oxidoreductase
SCO5261	0.2	−0.2	−0.6	0.0	−0.1	0.8	−0.7	−1.5	Putative malate oxidoreductase
SCO2494	1.1	1.2	−5.1	−3.1	−0.1	0.4	−3.9	−4.3	Putative pyruvate phosphate dikinase
SCO4827	0.2	−0.5	−0.3	0.3	−0.3	0.4	0.1	−0.5	Mdh Malate dehydrogenase
SCO4979	−0.2	5.7	0.1	−3.1	0.0	4.0	0.6	−4.9	PckG Phosphoenolpyruvate carboxykinase (PEPCK)
SCO5047	4.6	2.3	−3.2	−0.6	0.5	4.2	1.6	−2.3	GplX Fructose-1,6-bisphosphatase
Pentose phosphate pathway									
SCO1942	−0.9	−0.8	1.6	1.3	−0.6	−0.1	0.0	−0.7	Pgi2 Glucose 6-phosphate isomerase 2
SCO1937	−1.5		1.1		−0.5	−1.0	−0.2	0.5	Zwf2 Glucose 6-phosphate 1-dehydrogenase
SCO1939	−0.9	−0.5	0.4	0.9	−0.6	−0.7	0.2	0.1	Pgl DevB 6-phosphogluconolactonase
SCO0975	0.8	1.5	−0.4	−0.4	0.5	1.1	0.1	−1.0	Zwf3 6-phosphogluconate dehydrogenase
SCO3877	−1.7	−1.4	1.4	1.2	−0.2	−1.6	−0.4	1.2	Putative 6-phosphogluconate dehydrogenase
SCO1464					−0.3	−0.2	0.0	−0.2	Rpe Ribulose-phosphate 3-epimerase
SCO2627	1.4	0.6	−0.6	0.1	−0.3	0.9	1.0	−0.6	Putative sugar-phosphate isomerase
SCO1935	0.4	−0.5	−0.3	0.6	0.0	−0.4	0.1	0.4	TktA1 Transketolase A
SCO1936	−0.4	−0.4	−0.1	0.6	0.2	−0.2	0.2	0.5	Tal2 Transaldolase 2
SCO6659	−1.5	−0.4	3.3	2.5	0.3	0.3	1.9	1.6	Pgi1 pgi Glucose 6-phosphate isomerase 1
SCO6661	0.3	−1.1	0.1	2.5	0.2	0.1	2.3	2.1	Zwf Glucose 6-phosphate 1-dehydrogenase
SCO6658	−0.1		1.2						6-phosphogluconate dehydrogenase
SCO6660	0.1	−1.0	1.6	2.3	0.7	−0.6	1.4	2.7	Putative uncharacterized protein
SCO6663	−1.5	−1.4	2.9	2.6	0.4	0.1	2.0	2.4	TktB Transketolase B
SCO6662	−0.5	−1.5	2.4	3.1	0.8	0.2	2.3	2.8	Tal1 Transaldolase 1

a. Quantitative proteomic comparison of *glkA* deletion strain and parent strain (M145). Strains were grown in the presence of mannitol (M), glucose (G), and/or fructose (F), as indicated (see Fig. 1). The comparison between strains is indicated as ratios of Δ*glkA*/M145.

b. Proteins that demonstrate glucose repression/stimulation in the parent strain (^{2}log ratio < -1 or > 1, respectively, in the presence of mannitol, fructose, or both) are indicated in bold. In case glucose regulation was not relieved in the *glkA* deletion mutant (^{2}log ratio still < -1 or > 1, with same sign), proteins are also underlined.

c. Results are given as ^{2}log ratio, therefore positive number indicate upregulation and negative numbers downregulation respectively. No ratio is provided in case less than three quantification events were available.

© 2012 Blackwell Publishing Ltd,

enzyme in gluconeogenesis which hydrolyses fructose-1,6-bisphosphate to fructose-6-phosphate, demonstrated typical Glk-dependent CCR. However, expression of GlpX was massively upregulated in the *glkA* mutant in mannitol-grown cultures.

Other enzymes in the anaplerotic node subject to weak Glk-dependent CCR were the two malic enzymes (SCO2951, SCO5261). Interestingly, repression of NADH generating SCO2951 (Rodriguez *et al*., 2012) was stronger in mannitol-grown cultures, while repression of NADPH generating SCO5261 was stronger in fructose-grown cultures. This might reflect the need for more NADPH to produce secondary metabolites under nutrient-limiting conditions. Finally, the expression pattern of pyruvate carboxylase (pyc; SCO0546), converting pyruvate to oxaloacetate, also followed Glk-dependent CCR suggesting that this enzyme does not have an anaplerotic function in *S. coelicolor*, but may rather be involved in converting NADH to NADPH using malate dehydrogenase and malic enzyme (Sauer and Eikmanns, 2005), which is supported by the very similar expression pattern of Pyc, malate dehydrogenase (SCO4827) and NADP-dependent malic enzyme (SCO5261).

All enzymes in gluconeogenesis demonstrated Glk-dependent expression with exception of pyruvate phosphate dikinase (PPDK; SCO2494), which directly generates PEP from pyruvate, the opposite of the reaction catalysed by pyruvate kinase. This enzyme belonged to those most strongly repressed by glucose (8- to 35-fold), both in wild-type and *glkA* mutant cells. PPDK is the only identified protein that is massively downregulated by glucose independent of GlkA in both mannitol and fructose-grown cultures. This suggests a key role for PPDK in Glk-independent carbon control in streptomycetes.

From glucose to NADPH: the pentose phosphate pathway. The oxidative part of the pentose phosphate pathway (PPP) uses glucose to produce ribulose-5-phosphate and the reducing equivalent NADPH, which is used for reductive biosynthesis reactions. Ribulose-5P is then converted in the non-oxidative part of the pathway to other pentoses, such as ribose-5P for incorporation into nucleotides. The non-oxidative part can also generate intermediates for glycolysis/gluconeogenesis as to utilize pentose sugars as energy source. There are two clusters encoding the majority of enzymes of the PPP in *S. coelicolor*, namely SCO1935-1942 and SCO6658-6663. Considering the chromosomal location, SCO6658-6663 is considered as the secondary PPP cluster and may be involved in providing NADPH for secondary metabolite production (Challis and Hopwood, 2003). The expression profiles indicated that the PPP enzymes are induced by glucose in both wild-type and *glkA* mutant cells, but in the absence of Glk activity their expression was reduced in comparison to that in the parental strain M145 (Table 1). In particular, the secondary cluster showed on average four to eightfold induction by glucose in a Glk-independent manner. PPP enzymes located outside the two major clusters, such as 6-phosphogluconate dehydrogenase (SCO0975, SCO3877), ribulose-5-P isomerase (SCO2627), and ribulose-5-P epimerase (SCO1464), demonstrated expression profiles that differed from the expression changes described above for the two clusters, indicating alternative regulation of expression for these proteins.

Carbon catabolite repression and inducer exclusion

An important mechanism in the control of carbon utilization is inducer exclusion, i.e. repression of the internalization of less preferred carbon sources to prevent induction of the utilization operons. 70 proteins showed typical CCR, namely downregulated at least twofold in M145 by glucose and upregulated in *glkA* mutants in glucose; 60 occasions were seen in fructose-grown cultures and 16 in mannitol-grown cultures. Six of those were found in both (Table S4).

In terms of the PTS, the fructose utilization proteins FruK (fructokinase) and FruA (fructose permease) and its regulator FruR were strongly repressed by glucose and enhanced in the *glkA* mutant (Table 2). Interestingly, the general components of the PTS (Brückner and Titgemeyer, 2002) were differentially expressed. While there was no change in the expression of EI (SCO1391) or $EIIA^{Crr}$ (SCO1390) under any of the conditions nor in the *glkA* mutant, HPr (SCO5841), was upregulated around twofold in the presence of glucose when fructose was also present and in both M145 and its *glkA* mutant. This effect was not observed in the presence of mannitol. One other PTS component was identified (NagF, SCO2905), which is required for N-acetylglucosamine (GlcNAc) transport (Nothaft *et al*., 2010). The GlcNAc metabolic enzymes NagK, NagA and NagB, which are important for the GlcNAc-mediated control of antibiotic production (Swiatek *et al*., 2012b), were not detected, most likely as result of lack of induction in the absence of N-acetylglucosamine.

By controlling the expression of MsiK, a universal transport ATPase that provides energy to many ABC transport systems in streptomycetes (Schlösser *et al*., 1997; Titgemeyer *et al*., 2007; Davidson *et al*., 2008), CCR targets a central protein in sugar transport. Other sugar-related transport systems that were subject to CCR in a GlkA-dependent manner were the likely mannitol transporter (SCO1898-1901), SCO6005, and the glycerol transporter (SCO1658-161). Most probably as a result of the lack of inducer, most other sugar transporters were not identified or did not show a typical CCR patterns, such as the

Table 2. Primary targets of glucose repression/stimulation.

Strain[a]	Δ*glkA*/M145	Δ*glkA*/M145	Δ*glkA*	M145	Δ*glkA*/M145	Δ*glkA*/M145	Δ*glkA*	M145	
Condition	M	GM	GM/M	GM/M	F	GF	GF/F	GF/F	Known or predicted function
Sugar importP									
SCO1391	0.1	–0.4	0.3	0.2	0.0	0.2	0.0	–0.3	PtsI crr Phosphoenolpyruvate-protein phosphotransferase
SCO5841	–0.6	–0.3	0.4	–0.2	0.4	0.6	1.1	1.2	PtsH Phosphocarrier protein HPr
SCO1390	0.4		0.0		–0.3	0.5	0.6	0.0	Crr, PTS system sugar phosphotransferase component IIA
SCO2905	0.6	–0.6	–0.8	1.6	0.2	–0.6	–0.6	0.3	NagF
SCO3196	0.4	4.7	0.1	–3.2	0.0	1.3	0.1	–1.2	FruA, fructose-specific permease
SCO3197	0.0	3.8	0.4	–1.8	–0.1	1.4	0.3	–1.2	FruK, Putative 1-phosphofructokinase
SCO3198	0.9		–0.6		–0.4	1.4	0.2	–1.9	FruR, deoR-family transcriptional regulator
SCO4240	0.7	1.4	–1.0	–0.9	0.3	0.9	0.5	–0.9	MsiK ABC transporter ATP-binding protein
SCO1658	–3.3		0.1			–0.3		–0.7	GylR Glycerol operon regulatory protein
SCO1659	–3.4	–1.4	–0.3	–2.4	0.8	2.4	–1.4	–1.8	GlpF GylA Probable glycerol uptake facilitator protein
SCO1660	–3.8	–1.5	0.0	–2.0	–1.2	0.5	0.1	–1.4	GlpK1 Glycerol kinase 1
SCO1661	–4.7	–2.6	–0.1	–1.6	0.0	–1.1	–0.8	–0.1	Putative glycerol-3-phosphate dehydrogenase
SCO1897	–0.9	1.7	0.2	–2.0		0.9		–2.1	Putative transcriptional regulator
SCO1898	–0.1	2.6	–0.2	–2.2					Putative substrate-binding protein
SCO1900	–1.3		1.0						Putative integral membrane sugar transport protein
SCO1901	–1.6	2.4	0.8	–2.4	0.2	2.5	–1.7	–4.4	Putative zinc-binding dehydrogenase
SCO6005	0.0		–1.1		0.7	1.2	–0.4	–1.2	sugar-binding lipoprotein
SCO6008	–0.4	2.3	3.8	1.2	0.8	2.9	2.6	0.5	Rok7B7 Probable transcriptional repressor protein
SCO6009	0.4	2.2	3.2	2.0	–0.1	2.0	1.8	0.1	XylF, xylose-binding protein
SCO6010	1.4	1.6	3.3	2.2	–0.1	0.8	2.0	1.0	XylG, ABC-transport system ATP-binding protein
SCO6011	0.9	1.5	2.6	2.7	0.0	2.7	3.0	0.7	XylH, ABC-type transmembrane transport protein
Amino acid utilization									
SCO2008	0.3	1.9	–0.5	–0.7	0.2	0.9	–0.4	–1.3	branched chain amino acid-binding protein
SCO2010	0.7	1.6	–1.0	–0.5	–0.1	0.4	–0.8	–1.1	branched chain amino acid transport permease
SCO2011	0.0	1.6	–0.2	–0.3	0.2	1.0	–0.3	–1.2	branched chain amino acid transport ATP-binding protein
SCO2012	–1.3	1.0	0.8	–0.3	–0.2	2.9	0.9	–1.5	branched chain amino acid transport ATP-binding protein
SCO3815	1.0	1.4	0.1	0.1	–0.6	0.8	0.2	–1.3	BkdC1 Dihydrolipoamide acyltransferase component
SCO3816	1.3	1.3	–0.8	–0.6	–1.1	–0.6	–0.3	–2.0	BkdB1 Branched-chain alpha keto acid dehydrogenase E1 beta subunit
SCO3817	0.6	1.9	–0.1	–0.5	–1.1	1.3	0.0	–1.9	BkdA1 Branched-chain alpha keto acid dehydrogenase E1 alpha subunit
SCO4089	0.2	2.3	0.7	–0.6	–0.8	2.3	1.0	–1.9	Vdh Valine dehydrogenase (ValDH)
SCO1454	3.1		–0.3		0.9	3.6	0.8	–2.7	Putative amino oxidase
SCO1455	3.5		–1.4		0.6	3.3	0.1	–2.3	Putative hydrolase
SCO1459					1.4	3.8	–0.5	–3.0	Putative amino acid transporter
SCO4397	–0.2		–0.2		–0.4	2.0	0.5	–1.3	Putative ABC transport system ATP-binding protein
SCO5774	–0.3		–0.2		0.2	–0.5	–1.1	–0.5	GluD Glutamate permease
SCO5775	–1.7		1.4		–0.1	2.4	1.6	–0.9	GluC Glutamate permease
SCO5776	–0.2	0.9	–0.2	–0.5	0.0	1.0	0.5	–0.6	GluB Glutamate-binding protein
SCO5777	–0.5	1.0	0.2	–0.4	0.3	1.2	0.6	–0.5	GluA Glutamate uptake system ATP-binding protein
Glutamate and nitrogen metabolism									
SCO4159	4.6		–3.7						GlnR Transcriptional regulatory protein
SCO5676	1.3	1.0	–0.5	–0.9	0.0	2.3	0.3	–2.2	GabT Putative 4-aminobutyrate aminotransferase
SCO2025	–1.8	–2.9	0.2	1.8	1.3	–2.5	0.1	3.7	GltD Putative glutamate synthase small subunit
SCO2026	–2.1	–3.4	0.0	1.8	0.7	–2.3	0.1	2.9	GltB Putative glutamate synthase large subunit
SCO4683	–1.7	–2.7	0.2	0.6	–0.2	–1.6	0.1	1.5	GdhA Glutamate dehydrogenase
SCO5498	–0.7	0.0	0.9	1.5	1.0	–2.1	–1.6	1.3	GatC Glutamyl-tRNA(Gln) amidotransferase subunit C
SCO2999	–0.1	2.4	–0.3	–1.0	–0.5	2.3	0.5	–2.5	Putative Glutamate dehydrogenase
SCO5976[b]	–0.3	–1.2	–1.2	0.0	1.2	–2.6	–2.8	0.8	ArgF arcB Ornithine carbamoyltransferase
SCO7036	–2.1	–1.3	0.7	0.1	1.7	–2.4	–2.8	1.2	ArgG Argininosuccinate synthase
SCO1570[b]	–1.6	–1.4	0.0	–0.2	2.0	–2.5	–3.8	0.8	ArgH Argininosuccinate lyase (ASAL)
SCO5975	0.2		–0.8						ArcA2 Arginine deiminase (ADI)
SCO1576					0.4	–0.7	–1.0	0.2	ArgR Arginine repressor
SCO1577	–2.0	–0.9	0.9	–0.2					ArgD Acetylornithine aminotransferase (ACOAT)

Table 2. *cont.*

Strain[a]	Δ*glkA*/M145	Δ*glkA*/M145	Δ*glkA*	M145	Δ*glkA*/M145	Δ*glkA*/M145	Δ*glkA*	M145	
Condition	M	GM	GM/M	GM/M	F	GF	GF/F	GF/F	Known or predicted function
SCO1579[b]	–1.4	–1.2	–0.2	–0.3	1.6	–2.3	–3.1	0.5	ArgJ Glutamate N-acetyltransferase
SCO1580	–1.6	–1.9	0.2	–0.1	1.3		–3.6		ArgC N-acetyl-gamma-glutamyl-phosphate reductase (AGPR)
SCO1222	2.7		–2.3		1.4	3.5	0.0	–2.1	Putative uncharacterized protein
SCO1223	2.2		–2.3		1.6	3.4	–0.1	–2.4	RocD Ornithine aminotransferase
SCO5520	1.6	1.1	0.0	–0.1	–0.1	1.1	0.3	–1.0	Delta-1-pyrroline-5-carboxylate dehydrogenase
SCO2770	1.1		–0.6		0.1	1.5	–0.2	–1.7	SpeB Agmatinase
Other amino acids									
SCO1773	1.9	1.3	–0.4	–0.1	0.3	2.1	0.4	–1.3	Alanine dehydrogenase
SCO2769	0.6		–0.1		–0.2	2.1	0.9	–1.3	Putative acetolactate synthase
SCO5512	0.2	–1.3	–0.5	1.0	0.6	–1.1	–0.8	1.2	IlvB Acetolactate synthase
SCO5514/SCO7154	–0.6	–1.1	–0.3	0.9	0.2	0.0	0.2	0.5	IlvC1/2 Ketol-acid reductoisomerase
SCO3406	–0.2	0.2	0.0	0.2		–3.7		2.9	TilS tRNA(Ile)-lysidine synthase
SCO2528	–1.5	–1.6	0.4	0.7	0.0	–1.3	0.0	1.8	LeuA 2-isopropylmalate synthase
SCO5522	0.2	–2.7	–1.9	1.3	1.0	–1.1	1.0	2.0	LeuB 3-isopropylmalate dehydrogenase
acyl-CoA									
SCO1174	0.0	0.2	–1.0	–1.5	–1.5	2.5	0.3	–3.3	ThcA Probable aldehyde dehydrogenase
SCO1428	0.7	2.8	0.2	–1.8	–0.4	2.0	–0.1	–2.4	Acd Acyl-CoA dehydrogenase
SCO1814	–0.7	0.3	0.9	–0.4	–0.8	1.3	1.5	–0.6	InhA Enoyl-[acyl-carrier-protein] reductase [NADH]
SCO1838					–0.4	0.3	–0.2	–0.7	enoyl-CoA hydratase/isomerase
SCO2774	0.5	1.3	–0.4	–0.9	–0.2	0.3	–0.3	–0.7	AcdH2 Acyl-CoA dehydrogenase
SCO2776	0.5	2.8	0.2	–0.8	1.6	1.9	–0.3	–0.9	AccD1 Acetyl/propionyl CoA carboxylase, beta subunit
SCO2777	0.5	3.3	0.1	–1.6	1.5	2.1	–0.3	–0.9	AccC Acetyl/propionyl CoA carboxylase alpha subunit
SCO2778	–0.3		0.6		1.2	2.9	0.4	–1.1	HmgL Hydroxymethylglutaryl-CoA lyase
SCO2779	–0.6	3.1	0.7	–1.4	1.6	1.8	0.0	–0.6	AcdH Acyl-CoA dehydrogenase
SCO3563	–0.5	–0.2	–0.3	–0.4	0.2	0.7	–0.1	–0.3	AcsA Acetyl-coenzyme A synthetase
SCO4800	–0.7	0.4	0.7	–0.5					IcmB Isobutiryl CoA mutase, small subunit
SCO4930	1.0	1.9	–0.7	–1.8	0.7	0.7	–0.4	–0.5	Putative enoyl-CoA hydratase
SCO5399	–0.3	0.8	0.4	–0.1	–0.2	1.0	–0.1	–1.2	Probable acetoacetyl-coA thiolase
SCO5415	0.7	3.5	0.1	–2.2	–1.4	1.0	0.4	–2.0	IcmA Isobutyryl-CoA mutase A
SCO5459	0.7	1.1	0.6	–0.5	0.2	0.5	0.3	–0.4	Putative enoyl-coA hydratase
SCO5679	1.5	0.8	–0.3	–0.6	–0.1	2.3	0.4	–1.8	Putative aldehyde dehydrogenase
SCO6195	–0.2		–1.1		0.0	1.5	0.1	–1.2	Macs1 acyl-coenzyme A synthetase
SCO5515	–0.4	–2.0	–0.4	0.8	0.5	–1.6	–0.2	2.0	SerA Probable D-3-phosphoglycerate dehydrogenase

a. ^{2}log ratios of protein levels under the indicated conditions. See footnotes of Table 1.
b. SCO1570, SCO1579 and SCO5976 were repressed by glucose in the *glkA* mutant but not significantly altered in the parental strain. They have been marked in blue in Fig. 2.

well-studied maltose-binding protein MalE (SCO2231) and the alpha-glucosidase AglA (SCO2228), which are controlled by the specific regulator MalR (van Wezel *et al.*, 1997a,b); levels of both proteins were enhanced in the *glkA* mutant, but not reduced in the presence of glucose in wild-type cells (Table S2).

Strikingly, the xylose transporter (SCO6009-6011) was up to eightfold upregulated in *glkA* mutants in glucose + fructose as compared with fructose alone, and also upregulated in Δ*glkA* relative to the parent M145 (Table 2). Interestingly, ROK7B7 (SCO6008) showed a very similar expression pattern, suggesting that Rok7B7 activates the SCO6009-6011 cluster. The only other ROK protein with clear expression level changes was ppgK (polyphosphate glucokinase, SCO5059), with a similar expression pattern as Rok7B7 and the xylose transporter proteins.

Inducer exclusion was not limited to sugar utilization, since also amino acid transporters demonstrated typical CCR (Table 2): The transporter for branched-chain amino acids, the ABC-transporters for glutamate (SCO5774-5777), for an unknown amino acid (SCO1454-1459) and for an ABC transporter ATP-binding unit with unknown substrate (SCO4397).

Amino acids, nitrogen metabolism and the urea cycle

Glutamate is preferred as a carbon source over glucose in *S. coelicolor*, with all glutamate utilized before glucose utilization starts (van Wezel *et al.*, 2006). Nevertheless, glutamate uptake was subject to Glk-dependent CCR, with expression of subunits of glutamate synthase (SCO2025-2026) was around eightfold induced by glucose in the wild-type strain and fivefold downregulated in Δ*glkA*

(Table 2, Fig. 2C). Glutamate dehydrogenase (GdhA) provides an alternative synthesis pathway; two copies exist, which showed opposite control, with Glk-dependent glucose induction for SCO4683, and glucose repression of SCO2999, indicating that the latter might effect the utilization of glutamate as energy source. Other enzymes acting on glutamate, 4-aminobutyrate aminotransferase and glutamyl-tRNA(Gln) amidotransferase, also demonstrated expression levels that were dependent on glucose and Glk, as they were repressed and induced by glucose respectively. There was a massive 25-fold increase of the global nitrogen regulator GlnR (SCO4159) in Δ*glkA* in mannitol-grown cultures. However, GlnR expression was repressed by glucose in the *glkA* mutant.

Glutamate is the starting point for the conversion to arginine and fumarate via the urea cycle (Fig. 2C), and this pathway (SCO5976, SCO7036 and SCO1570) was activated by the addition of glucose to fructose-grown cultures, while in *glkA* mutant cells, these proteins were downregulated around 10-fold by glucose, indicating additional Glk-independent carbon control (Table 2). The arginine repressor (ArgR, SCO1576) and enzymes converting glutamate to the urea cycle-intermediate ornithine (SCO1577-1580) demonstrated a very similar expression pattern. In contrast, SCO1223 and SCO5520 were subject to Glk-dependent CCR, suggesting they catalize the conversion from ornithine to glutamate.

Glk-dependent CCR and the control of development

The so-called *bld* mutants are pleiotropically defective in the initiation of development, and are typically defective in CCR as well as antibiotic production (Pope *et al*., 1996). Expression of BldB (SCO5723), BldM (SCO4768) and BldN (SCO3323) was repressed by glucose in the *glkA* deletion mutant (Table 3). A direct role for BldB in CCR was previously suggested (Pope *et al*., 1998), while BldN is a developmental sigma factor that controls early and late developmental genes, with among others *bldM* as a direct target (Bibb *et al*., 2000). The latter is highlighted by the similar expression profiles of BldN and BldM. BldD (SCO1489), a pleiotropic regulator of developmental genes (den Hengst *et al*., 2010), and BldG (SCO3549) showed reduced expression in the *glkA* mutant, while BldC demonstrated Glk-dependent glucose induction in mannitol-grown cultures. The sporulation control protein WhiA (SCO1950) was virtually unchanged in all samples.

Interestingly, all 26 proteins identified in the region SCO0167-0260 conformed to the same expression pattern (Table S2). The genes for these proteins lie around the two-component regulatory system SCO0203 and SCO0204 (forming the sensory kinase and response regulator respectively; Wang *et al*., 2009), and are likely controlled by them (van Rossum *et al*., unpubl. data).

Table 3. Carbon source dependent expression profiles on development-related proteins and selected regulators.

Strain[a]	Δ*glkA*/M145	Δ*glkA*/M145	Δ*glkA*	M145	Δ*glkA*/M145	Δ*glkA*/M145	Δ*glkA*	M145	
Condition	M	GM	GM/M	GM/M	F	GF	GF/F	GF/F	Known or predicted function
SCO0168					2.6	3.6	0.6	–1.6	Possible regulator protein
SCO0608	3.4		–1.0		2.2	0.8	–1.1	0.6	SlbR, regulatory protein
SCO0803						–2.5		1.4	RNA polymerase sigma factor
SCO0977	0.2		0.1		6.7		–9.1		Putative uncharacterized protein
SCO1078					2.5		–4.6		Putative lacI-family transcriptional regulator
SCO1489	–0.8	–0.8	0.6	–0.1	0.0	0.1	0.2	–0.2	BldD
SCO3075	–1.8	1.8	0.7	–1.1	–1.7	0.0	–0.2	–1.9	Putative transcriptional regulator
SCO3323	2.1		–1.5						BldN, RNA polymerase sigma factor
SCO3549	–2.1	0.2	2.0	0.1	–0.4	–0.6	–0.5	–0.4	RsbV bldG Anti-sigma-B factor antagonist
SCO4091	0.7	–1.1	0.0	2.6	–0.8	–0.8	–0.2	–1.5	BldC
SCO4768	2.2		–2.1						BldM, two-component regulator
SCO5112	0.5		–1.0		0.0	–1.7	0.4	0.7	BldKA putative ABC transport system integral membrane protein
SCO5113	–1.1	0.2	1.4	–0.1	–0.4	0.1	0.4	–0.3	BldKB putative ABC transport system lipoprotein
SCO5114	0.1	–0.2	–0.2	–0.2	–1.0	–0.1	0.2	–0.5	BldKC putative ABC transport system integral membrane protein
SCO5115	0.1	–0.4	–0.3	0.1	–0.7	–0.4	0.1	–0.2	BldKD putative ABC transporter intracellular ATPase subunit
SCO5116	0.2	–0.1	–0.1	0.0	–0.4	–0.8	–0.3	0.0	BldKE Putative peptide transport system ATP-binding subunit
SCO5243	–1.4		–0.8		–0.9	1.4	1.0	–1.3	SigH, RNA polymerase sigma factor
SCO5723	2.1		–1.4		0.4	–0.3	–0.5	0.1	BldB

a. ^{2}log ratios of protein levels under the indicated conditions. See footnotes of Table 1.

Amazingly, the majority of the proteins that were most strongly (17- to 80-fold) enhanced in *glkA* null mutants in mannitol-grown cultures belong to this group. Their expression was repressed by glucose in a Glk-dependent manner. Other pleiotropic regulators with similar expression pattern as SCO0204 included the nitrogen regulator GlnR (Table 2) and the γ-butyrolactone receptor protein SCO0608 (Table 3) (Yang *et al*., 2012), which represses *scbRA* expression (see below). The expression of Crp (SCO3571), the global regulator of germination and early vegetative processes protein (Piette *et al*., 2005), was unchanged (Table S2). The same was true for DasR (SCO5231), the pleiotropic regulator of the N-acetylglucosamine metabolism, PTS transport and antibiotic production (Rigali *et al*., 2008; Swiatek *et al*., 2012a), which explains the moderate response of the *nag*/*pts* regulon.

Carbon source-dependent control of antibiotic production

The gene cluster for the production of prodigionins (collectively indicated as Red) in *S. coelicolor* runs from SCO5877-5898 (Feitelson *et al*., 1985; Bentley *et al*., 2002). Expression of at least SCO5884 was subject to typical glucose repression, while all expression was strongly reduced in the *glkA* mutant relative to M145 in mannitol-grown cultures, with 15–70-fold downregulation (Table 4). The proteins were not detected, and most likely not expressed at this early time-point for antibiotic production, in fructose-grown cultures. Although secondary metabolite production was not yet observable at mid-exponential growth phase, this protein expression pattern corresponded remarkably well to the levels of prodiginin production found by MALDI-ToF mass spectrometry after growth became stationary (Fig. S1): repressed by glucose and by deletion of *glkA*. Proteins of the biosynthetic machinery for calcium-dependent antibiotic (CDA) showed similar response, with glucose repression and strong reduction of expression (6–16-fold) in Δ*glkA* in mannitol-grown cultures (17 proteins identified, including the three peptide synthetases SCO3230-3232).

Expression of biosynthetic proteins of the Type I modular PKS for Cpk was highly divergent between wild-type an *glkA* mutant. Addition of glucose to mannitol-grown cultures led to massive (6–40-fold) glucose repression of the Cpk proteins in the *glkA* mutant relative to the parent M145, with SCO6272-6284 all identified (Table 4). Under these conditions the expression of the Cpk enzymes was co-ordinated with the γ-butyrolactone Scb1 synthetase ScbA (SCO6266) and the *scbA* transcriptional activator ScbR, with around 100-fold reduced expression of ScbA in the *glkA* mutant. In other words, ScbA expression is completely dependent on an active Glk under these growth conditions. Experiments performed in fructose-grown cultures showed the mirror image, with stimulation of Cpk expression by glucose in *glkA* mutants relative to M145. ScbA and ScbR could not be quantified under these conditions. The only other proteins whose expression showed good correlation with Cpk were those encoded by the SCO1087-1089 operon conserved in streptomycetes, for a putative threonine aldolase, a short-chain dehydrogenases/reductase and a protein of unknown function respectively (Table S2).

SCO0608 (SlbR) was recently identified as a novel γ-butyrolactone receptor protein that directly controls *scbRA* expression and thereby functions as a repressor of antibiotic biosynthesis (Yang *et al*., 2012). It followed a more or less inversed response, and is strongly upregulated in the *glkA* mutant (Table 3). This increase at least in part explains the strong reduction in ScbRA expression in the *glkA* mutant. The Cpk enzyme expression pattern was also opposite to that of SCO0977, a putative signalling N-acyl-transferase, and of enzymes for Arginine catabolism (urea cycle). The importance of these correlations awaits further elucidation.

We failed to detect any of the proteins encoded by the *act* cluster for actinorhodin biosynthesis, which is most likely due to the fact that Act production is switched on during transition phase (Gramajo *et al*., 1993), while our samples were taken during mid-exponential phase. Proteins for hopanoid biosynthesis (SCO6759-6771; nine out of 13 proteins identified) were unchanged under all conditions, while the siderophore coelichelin (SCO0489-0499; five out of 11 proteins identified) was enhanced in the *glkA* mutant but not affected by glucose.

Precursor supply for fatty acids and polyketide antibiotics. Many of the CCR-controlled genes related to precursors supply for fatty acid and polyketide metabolism (Table 2). They all demonstrated GlkA dependent CCR, although the degree of repression varied. We identified subunits of the acetyl-CoA carboxylase complex (AccC and AccD), acyl-CoA dehydrogenases (AcdH1, AcdH2 and Acd), enoyl-CoA hydratases (SCO1838, SCO4930 and SCO5459), isobutyryl-CoA mutases (IcmB and IcmA), enoyl-ACP reductase (InhA), Hydroxymethylglutaryl-CoA lyase (HmgL), acetoacetyl-coA thiolase (SCO5399), and ac(et)yl-CoA synthetases (AcsA and Macs1). Acetyl-CoA carboxylase produces malonyl-CoA (Tong, 2005), which is a substrate for the biosynthesis of fatty acids and important for antibiotic production in *Streptomyces* (Rodriguez *et al*., 2001), while acetyl-CoA dehydrogenase and enoyl-ACP reductase effect the saturation of fatty acids (Thorpe and Kim, 1995) and (polyketide) antibiotics. Enoyl-CoA hydratase hydrates the double bond between the second and third carbon of acyl-CoA and is required for the metabolism of fatty acids to produce Acetyl-CoA and energy, while isobutyryl-CoA mutase converts

Table 4. Synthesis of secondary metabolites.

Strain[a]	Δ*glkA*/M145	Δ*glkA*/M145	GlkA	M145	Δ*glkA*/M145	Δ*glkA*/M145	Δ*glkA*	M145	
Condition	M	GM	GM/M	GM/M	F	GF	GF/F	GF/F	Known or predicted function
Cryptic polyketide (CPK)									
SCO6265		–3.7		0.6					ScbR Gamma-butyrolactone-binding protein
SCO6266		–6.6		–1.1					ScbA protein, Scb1 synthetase
SCO6272		–4.2		–1.1	–3.5		2.2		Putative secreted FAD-binding protein
SCO6273		–2.8		–0.7	–3.0	0.5	0.2	–3.1	Putative type I polyketide synthase
SCO6274	–0.9	–2.3	1.9	–0.9	–2.8	0.4	0.3	–3.2	Putative type I polyketide synthase
SCO6275	–0.3	–3.1	–2.0	–0.7	–2.8	1.1	0.5	–3.1	Putative type I polyketide synthase
SCO6276		–4.1		–0.5	–3.6	2.2	1.1	–4.6	Putative secreted protein
SCO6277		–3.0		–0.5	–3.5	0.9	0.6	–3.3	Putative epoxide hydrolase
SCO6278		–3.9		–0.2	–3.3	0.5	0.9	–2.9	Putative integral membrane transport protein
SCO6279	–0.5	–4.6	–2.5	–0.4	–3.2	1.6	0.8	–3.8	Putative diaminobutyrate-pyruvate aminotransferase
SCO6281		–2.2		–0.8					Putative FAD-binding protein
SCO6282	0.4	–5.3	–3.8	0.6	–3.9	1.9	1.1	–4.5	Putative 3-oxoacyl-[acyl-carrier protein] reductase
SCO6283	–0.5	–4.1	–2.3	0.3	–3.9	3.4	1.2	–5.8	Putative uncharacterized protein
SCO6284						1.0		–3.1	Putative decarboxylase
Prodigiosins (RED)									
SCO5878	–1.6		–0.1						RedX Polyketide synthase RedX
SCO5879	–4.1		–0.3						RedW Acyl-coa dehydrogenase RedW
SCO5884	–6.0		0.8	–2.1					Putative uncharacterized protein
SCO5888	–4.8		1.3						FabH3 redP 3-oxoacyl-[acyl-carrier-protein] synthase 3
SCO5889	–5.0		0.6						RedO Putative uncharacterized protein
SCO5892	–3.5		–0.7						RedL Polyketide synthase
SCO5893	–4.0		–0.2						RedK Oxidoreductase
SCO5895	–3.8		0.2						RedI Putative methyltransferase
SCO5896	–4.8		1.4						RedH Phosphoenolpyruvate-utilizing enzyme
SCO5897	–6.2		1.1						RedG Putative oxidase
Calcium dependent antibiotic (CDA)									
SCO3228	–2.7		–0.5						Putative glycolate oxidase
SCO3229	–3.3		–0.5						Putative 4-hydroxyphenylpyruvic acid dioxygenase
SCO3230	–3.7		–0.1						CdaPSI CDA peptide synthetase I
SCO3231	–4.0	–0.1	–0.2	–2.0					CdaPS2 CDA peptide synthetase II
SCO3232	–3.6		–0.6						CdaPS3 CDA peptide synthetase III
SCO3233	–3.7	–0.7	–1.2	–2.2					Putative hydrolase
SCO3234	–3.2	–0.1	0.3	–2.0					HasP 3-hydroxyasparagine phosphotransferase
SCO3236	–3.3		–0.1		0.2		–1.2		AsnO L-asparagine oxygenase
SCO3238	–2.9		–0.4						Putative uncharacterized protein
SCO3241	–3.2		–0.8						Putaive isomerase
SCO3243	–3.3		–1.2						Putative myo-inositol phosphate synthase
SCO3247	–2.7	0.4	–0.2	–0.2					Putative acyl CoA oxidase
SCO3248	–3.6		–0.2						FabF3 Putative 3-oxoacyl-[acyl carrier protein] synthase II
Coelichelin									
SCO0492	1.3	1.3	–0.1	0.7	1.2	1.9	0.4	–0.5	Putative peptide synthetase
SCO0494	1.6	1.4	–0.5	0.7	0.5	0.9	0.9	0.4	Putative iron-siderophore-binding lipoprotein
SCO0498	1.5	1.8	–0.2	1.2	1.7	3.5	0.8	–0.7	Putative peptide monooxygenase
SCO0499	0.8	1.3	0.1	0.6	1.4	2.6	0.1	–0.7	Putative formyltransferase

a. ^{2}log ratios of protein levels under the indicated conditions. See footnotes of Table 1.
FAD, flavin adenine dinucleotide.

© 2012 Blackwell Publishing Ltd,

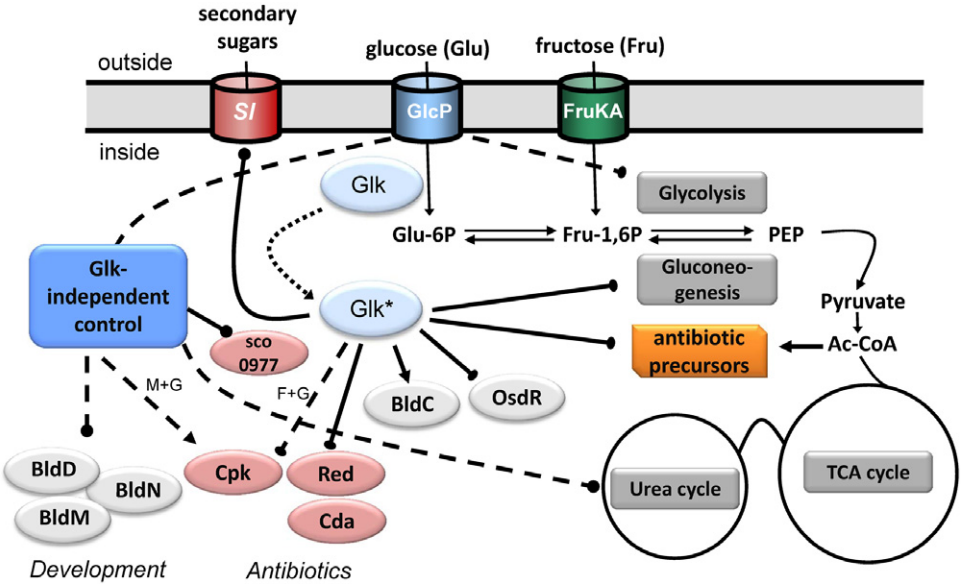

Fig. 3. Model for CCR in *S. coelicolor* during exponential growth. Glk-dependent (solid arrows) and Glk-independent (dashed arrows) glucose repression is shown for major metabolic routes, development and antibiotic production. Only responses in glucose-grown cultures are shown. Arrows indicate activation, bullets repression. Glk was previously proposed to be activated post-translationally (Glk*) in a glucose transport-dependent manner (van Wezel *et al.*, 2007). Cda, Cpk and Red refer to the biosynthetic proteins for production of the antibiotics calcium-dependent antibiotic, cryptic polyketide and undecylprodigiosin respectively. Cpk biosynthesis is activated in glucose + mannitol, and repressed in glucose + fructose. BldC, BldD, BldM and BldN are regulators of early development. Data are based on proteomics experiments performed on mycelia harvested during mid-exponential growth from liquid-grown cultures. SI, substrate induction. PEP, phosphoenolpyruvate.

2-methylpropanoyl-CoA into butanoyl-CoA, and both proteins relate to fatty acid as well as antibiotic biosynthesis (Patton *et al.*, 2000; Liu and Reynolds, 2001). Hydroxymethylglutaryl-CoA lyase and acetoacetyl-CoA thiolase interconvert acetyl-CoA, acetoacetate, and acetoacetyl-CoA, while, finally, ac(et)yl-CoA synthetases activate acyl chains for synthesis of fatty acids and polyketides.

In connection to this, CCR was also observed for branched chain amino acid uptake (SCO2008-2012, Table 2), valine dehydrogenase (Vdh), and the branched-chain amino acid dehydrogenase complex 1 (SCO3815-3817). The latter converts the branched chain amino acids Leu, Ile and Val into 3-methylbutanoyl-CoA, 2-methylbutaboyl-CoA, and isobutyryl-CoA, respectively, which serve as precursors for branched-chain fatty acid biosynthesis. These molecules also serve as starter units for the biosynthesis of antibiotics, exemplified by the polyketide avermectin in *S. avermitilis* (Marsden *et al.*, 1998).

Discussion

In this work we have applied an advanced proteomics approach that for the first time provides detailed insight into Glk-dependent and -independent control of gene expression in *S. coelicolor*. A model for CCR in *S. coelicolor* is presented in Fig. 3. We were able to compare over 2000 proteins between *S. coelicolor* M145 and its *glkA* mutant, and between cultures grown on different combinations of carbon sources. This allowed us to identify most of the cytoplasmic proteins that were expressed at detectable levels, and to study the changes in expression of almost all enzymes involved in glycolysis, TCA cycle, gluconeogenesis, the urea cycle, the anaplerotic node and the pentose phosphate pathway. A canonical target for Glk-dependent CCR conforms to the following expression profile in proteomics analysis: (i) expression repressed by glucose in M145, and unchanged in the *glkA* mutant; and (ii) Δ*glkA*/M145 ratio unchanged when grown on fructose or mannitol alone, and high values in the presence of additional glucose. Theoretically, in the *glkA* mutant there should be little difference in terms of carbon flux when glucose is added in addition to fructose. The changes should therefore reveal aspects of the regulatory role of Glk, or the induction by glucose independent of *glkA*. In total 68 and 146 targets were down- and upregulated more than twofold in the *glkA* mutant in response to glucose respectively. One consequence of the large horizontal comparisons and the huge data sets that need to be analysed was the choice of a specific time point for protein isolation. It should be noted that expression will vary between different growth phases, and in particular for antibiotic- and development-related proteins, and our conclusions relate primarily to mid-exponential growth in liquid-grown cultures, i.e. during active growth and metabolism.

In terms of central metabolism, glucose stimulates glycolysis as well as the pentose phosphate pathway. This signalling is most likely mediated via the glucose transporter GlcP, as expression was also stimulated by glucose in the *glkA* mutant. Expression of the glucose transporter GlcP itself was 50-fold upregulated. In the presence of the glycolytic intermediate fructose, glucose activation was mostly lost. In contrast to the glycolytic enzymes, enzymes of the TCA cycle hardly changed when glucose was added, possibly due to metabolism of non-carbohydrate carbon sources such as amino acids. However, import and metabolism of amino acids was clearly subject to inducer exclusion, rendering it more likely that the TCA cycle is not regulated by protein expression but by supply of metabolic intermediates. Gluconeogenesis was subject to strong Glk-mediated CCR. However, pyruvate phosphate dikinase (SCO2494), which produces PEP in a single step from pyruvate, was massively repressed (some 30-fold) by glucose in a Glk-independent manner. Considering its central position and very strong change in expression in response to glucose, this identifies PPDK as a possible key player in Glk-independent carbon control in streptomycetes. Interestingly, the secondary PPP enzymes, which are thought to be involved in supplying NADPH as reducing power for secondary metabolite production (Challis and Hopwood, 2003), were also very strongly upregulated by glucose, and in a Glk-independent manner.

Enzymes involved in amino acid metabolism and transport, and in particular the enzymes responsible for converting glutamate to fumarate and arginine via ornithine and the urea cycle (Arg enzymes; SCO1570-1580, SCO5976 and SCO7036), were strongly downregulated by glucose in the *glkA* mutant. Interestingly, their expression pattern was opposite to that of the enzymes responsible for the biosynthesis of the cryptic polyketide Cpk in fructose-grown cultures (discussed below). The top hit among proteins that were glucose repressed in the *glkA* mutant was SCO0977, an *N*-ac(et)yltransferase. The expression profile of this protein is rather bizarre, with 60-fold upregulation in *glkA* mutants in fructose-grown cultures, while addition of glucose led to 600-fold reduced expression. Since fructose is also present, glycolysis can proceed normally under these growth conditions. In mannitol-grown cultures its expression was similar in wild-type and *glkA* mutant, and addition of glucose had no effect. SCO0977 belongs to a family of signalling *N*-acyltransferases that is involved in acyl-CoA-dependent transfer of an acetyl-, succinyl or myristoyl group onto a substrate, and includes arginine/ornithine N-succinyltransferase, Myristoyl-CoA:protein N-myristoyltransferase and Acyl-homoserinelactone synthase. It is unclear why SCO0977 should be completely dependent on *glkA* specifically in fructose-grown cultures, but it is tempting to speculate that SCO0977 has a regulatory role in CCR via the post-translational modification of target proteins.

Carbon catabolite repression functions in the expected manner in respect of inducer exclusion (Fig. 3). Many proteins belonging to sugar and amino acid transporter systems, as well as the universal ABC transporter ATPase MsiK, were repressed by glucose in a Glk-dependent manner. A striking exception is the xylose transporter XylFGH (SCO6009-6011), the only sugar transport system detected that was strongly activated by glucose and in a Glk-independent manner, along with its putative ROK-family regulator Rok7B7, which is an activator of actinorhodin biosynthesis (Martinez *et al*., 2005; Park *et al*., 2009). Interestingly, deletion of *rok7B7* results in loss of CCR of agarase expression, implicating Rok7B7 directly in carbon catabolite control (M.A. Swiatek and G.P. van Wezel, unpubl. data). Therefore, the upregulation of Rok7B7 in the presence of glucose may be a compensatory effect, in an attempt to effect CCR in the absence of GlkA. Direct transcriptional control of *glkA* by Rok7B7 is less likely, as Glk expression is constitutive and probably independent on the carbon source, and Glk is activated in a post-translational manner (van Wezel *et al*., 2007); considering the strong phylogenetic linkage between *rok7B7* and the xylose operon, we anticipate that xylose or a derivative thereof serves as a ligand for Rok7B7. We are currently undertaking an extensive systems biology effort to elucidate the role of Rok7B7 in CCR and the role of the C5 sugar xylose.

The proteomics data revealed a spectacular and surprisingly differential effect of carbon utilization on antibiotic production (Fig. 3). CCR plays a crucial role in the expression of virulence genes, which often enable bacteria to access new sources of nutrients (Milenbachs *et al*., 1997; Shelburne *et al*., 2008). Perhaps the control of antibiotic production should also be seen in this light. Antibiotics are a defence mechanism, and at the same time destruction of the targeted microorganisms provides streptomycetes with new sources of nutrients in the nutrient-deprived soil. Like virulence, antibiotic production is subject to CCR. The antibiotic gene clusters showed highly co-ordinated expression, which also provides further validation for our proteomics procedure. The block in development and antibiotic production in many *bld* mutants is medium dependent, and restoration of these processes was achieved by the additional deletion of *glkA* (van Wezel and McDowall, 2011). This demonstrates very clearly the direct linkage between CCR on the one hand, and development and antibiotic production on the other. As for the biosynthetic proteins for CDA and Red production, glucose repression in the wild-type strain could be quantified for a few of the biosynthetic proteins and, at least for Red, correlated to actual production levels. Deletion of *glkA* effected a 10–15-fold reduction of the expres-

sion of almost all biosynthetic enzymes for CDA and Red in mannitol-grown cultures. This strongly suggests that antibiotic production is repressed by glucose in a *glkA*-dependent manner. The same was true for enzymes of the Type I modular PKS for Cpk biosynthesis in fructose-grown cultures. Conversely, expression of the Cpk biosynthetic proteins was subjected to Glk-independent CCR in mannitol-grown cultures. It was published previously that the control of the *cpk* cluster by the γ-butyrolactone Scb1 is complex (Takano *et al*., 2001; 2005). Scb1 is synthesized by ScbA, and acts as a ligand for ScbR, which is then released from its target, relieving *cpk* gene expression. Addition of glucose to a *glkA* null mutant in mannitol-grown cultures led to strong CCR of expression of the Cpk enzymes as well as of ScbRA, whereby ScbA expression was completely dependent on Glk. The co-ordinated expression of Cpk and ScbRA is surprising, since ScbR is thought to be the transcriptional repressor of *cpk* gene expression (Takano *et al*., 2001; 2005). Experiments performed in fructose-grown cultures showed the mirror image, with stimulation of Cpk expression by glucose in *glkA* mutants relative to M145. These data show that Glk not only plays an important role in the control of antibiotic production, but also that it is a far more complex relationship than suspected so far.

The effect of glucose on development may be explained by the reduced expression of several development-related regulatory proteins, including BldB, BldM and BldN, and most likely also by the strong activation of the stress-related response regulator SCO0204. Recent studies in our laboratory revealed that SCO0204 controls development and oxidative stress (van Rossum *et al*., unpubl. data), and activates genes required for early growth, while it represses developmental genes. Deletion of SCO0204 (renamed OsdR, for oxidative stress and development) accelerates development and actinorhodin production. Our interest in SCO0204 stems from its activity as a repressor of SsgB, which is essential for sporulation and required for the onset of sporulation-specific cell division (Keijser *et al*., 2003; Willemse *et al*., 2011). In mannitol-grown cultures the developmental inhibitor OsdR was strongly repressed by Glk, while SCO0204 was activated by glucose in wild-type cells and repressed in the *glkA* mutant. As mentioned above, this developmental block in most *bld* mutants is carbon-source dependent, and in particular blocked by glucose, while sporulation of the mutants is permitted on mannitol-containing agar plates; restoration of sporulation to *bld* mutants was observed following the deletion of *glkA* (van Wezel and McDowall, 2011). The repression of Bld proteins and activation of the development repressor OsdR provides important clues as to how glucose suppresses development.

Summarizing, our work reveals complex control of antibiotic production by glucose and Glk-dependent and Glk-independent CCR in primary and secondary metabolism. Clearly, glucose repression is far more complex than so far anticipated, whereby the control of several key CCR targets is governed in a Glk-independent manner. The extreme response of some yet unknown targets to changes in carbon utilization may provide new leads for the control of glucose repression in antibiotic-producing actinomycetes.

Experimental procedures

Strains and media

Streptomyces coelicolor A3(2) (Kieser *et al*., 2000) was obtained from the John Innes Centre strain collection. The *glkA* mutant derivative of *S. coelicolor* M145 has *glkA* replaced by the apramycin resistance cassette *aacC4*, and was made in the same way as (and simultaneously with) *S. coelicolor* M600 Δ*glkA* described previously (Barends *et al*., 2010). Strains were grown in 50 ml NMMP minimal medium with 0.5% (w/v) casamino acids (Kieser *et al*., 2000) supplemented with either 1% (w/v) mannitol; 0.5% glucose and 0.5% mannitol; 1% (w/v) fructose; or 0.5% glucose and 0.5% fructose as carbon source. Cultures were grown under vigorous shaking at 30°C. Cell growth was monitored by OD-measurement at 600 nm using a spectrophotometer (Starrcol standard, SC-60-S).

MALDI-ToF MS analysis

Mycelia were extracted with methanol and extract mixed 1:1 (v/v) with a saturated α-cyano-4-hydroxycinnamic acid solution in 50% (v/v) acetonitrile/0.05% (v/v) trifluoroacetic acid, 1 μl was spotted on a MALDI target plate, and samples were measured on a Bruker microflex LRF mass spectrometer in the positive ion reflectron mode using delayed extraction. For each spectrum, at least 1000 shots were acquired at 60 Hz.

Protein extracts

To prepare cell extracts, cells were washed twice and resuspended in sonication buffer (50 mM Tris pH 7.4, 5 mM $MgCl_2$, 40 mM NH_4Ac, 50 mM NaCl). Cells were sonicated and cell debris removed by centrifugation (16 000 *g*, 10 min, 4°C). Protein concentrations were determined using the Bradford-based Bio-Rad protein assay (Bio-Rad), measured on a Bio-Rad SmartSpec™ Plus at 595 nm, using BSA as a reference. Protein precipitation was performed according to protocol using chloroform/methanol precipitation (Wessel and Flugge, 1984).

Quantitative proteomics

Sample preparation. Fresh cultures were grown as indicated and samples were taken during mid-exponential growth phase, which was reached after 18–20 h after inoculation. Cell extracts were prepared and for each sample 0.33 mg of total protein was precipitated. Protein samples were digested with trypsin, in parallel, using in solution diges-

tion as follows: Proteins were dissolved in 180 µl 50 mM ammonium bicarbonate containing 0.1% (w/v) RapiGest SF Surfactant (Waters) and the sample was heated at 95°C for 5 min. DTT was added to a final concentration of 5 mM and the sample was incubated at 60°C for 30 min. Iodoacetamide was added to a final concentration 21.6 mM and the sample was placed in the dark for 30 min. Trypsin was added 1:100 (w/w) trypsin/protein and the sample was incubated o/n at 37°C. Digested peptides were acidified using formic acid to a final concentration of 1%, incubated at 37°C for 30 min, and spun down (20 000 *g*, 10 min) for Rapigest SF removal. Samples were dried using a vacuum concentrator and dissolved in 1 ml 5% formic acid.

Samples were labelled using stable isotope dimethyl labelling on-column using Ultra-Clean SPE C18 200 mg columns (Altech) as described (Boersema *et al*., 2009). Light medium, and heavy-labelled samples (0.33 mg each) were mixed as shown in Fig. 1A to yield 1 mg mixtures for fractionation.

Mixtures were dried using a vacuum concentrator, dissolved in ~ 1 ml 5% formic acid, and 0.5 ml was fractionated by cationic exchange (SCX) using a polysulfoethyl A column (PolyLC, 100 × 2.1 mm, particle size 5 µm, average pore size 200 Å, column volume 0.346 ml. Mobile phases were SCX A [10 mM KH_2PO_4, 20% (v/v) acetonitrile, pH 3] and SCX B [10 mM KH_2PO_4, 20% (v/v) acetonitrile, 0.5 M KCl, pH 3]. Peptides were separated using a gradient of 0–50% SCX B in 25 column volumes, followed by a gradient of 50–100% SCX B in 10 column volumes. The flow rate was set to 250 µl min^{-1}. In total, 26 peptide fractions were collected and LC-MS analysis was performed as indicated below.

LC-MS/MS analysis. Acidified peptides were desalted using StageTips (Rappsilber *et al*., 2007). To remove acetonitrile, samples were concentrated in a vacuum concentrator. Prior to LC-MS analysis, the volume was adjusted to 70 µl using a 3% (v/v) acetonitrile, 0.1% (v/v) formic acid solution.

Peptides were analysed on a Surveyor nanoLC system (Thermo, Waltham, MA) hyphenated to an LTQ-Orbitrap mass spectrometer (Thermo). Gold and carbon coated emitters (OD/ID = 360/25 µm tip ID = 5 µm), trap column (OD/ID = 360/100 µm packed with 25 mm robust Poros10R2/15 mm BioSphere C18 5 µm 120 Å) and analytical columns (OD/ID = 360/75 µm packed with 20 cm BioSphere C18 5 µm 120 Å) were obtained from Nanoseparations (Nieuwkoop, the Netherlands). The mobile phases [A: 0.1% (v/v) formic acid/H_2O, B: 0.1% (v/v) formic acid/acetonitrile] were made with ULC/MS grade solvents (Biosolve, Valkenswaard, the Netherlands). The emitter tip was coupled end-to-end with the analytical column via a 15 mm long TFE Teflon tubing sleeve (OD/ID 0.3 × 1.58 mm, Supelco, St Louis, MO) and installed in a stainless steel holder mounted in a nano-source base (Idex, Northbrook, IL).

General mass spectrometric conditions were as follows: an electrospray voltage of 1.6–2.0 kV was applied to the emitter, no sheath and auxiliary gas flow, ion transfer tube temperature 150°C, capillary voltage 20 V, tube lens voltage 110 V. Internal mass calibration was performed with air-borne protonated polydimethylcyclosiloxane (m/z = 445.12002) and the plasticizer protonated dioctylphthalate ions (m/z = 391.28429) as lock mass (Olsen *et al*., 2005).

For shotgun proteomics analysis, 10 µl of the samples was pressure loaded on the trap column with a 10 µl min^{-1} flow for 5 min followed by peptide separation with a gradient of 95 min 7–25% B, at a flow of 300 µl min^{-1} split to 250 nl min^{-1} by the LTQ divert valve. For each data-dependent cycle, one full MS scan (300–2000 m/z) acquired at high mass resolution (60 000 at 400 m/z, AGC target 1×10^6, maximum injection time 1000 ms) in the orbitrap was followed by five MS/MS fragmentations in the LTQ linear ion trap (AGC target 1×10^4, maximum injection time 50 ms for mixture 1 of the glucose vs mannitol measurement, 120 ms for the other mixtures) from the five most abundant ions. MS^2 settings were as follows: collision gas pressure 1.3 mT, normalized collision energy 35%, ion selection threshold of 750 counts, activation q = 0.25 and activation time of 30 ms. Fragmented precursor ions were dynamically excluded for 150 s and ions with $z < 2$ or unassigned were not analysed. Exclusion width was set to –1.5 Da to +3.5 Da for mixture 1 of the glucose vs mannitol experiment and –10 ppm to +10 ppm for the other mixtures.

Proteomics data analysis

Data analysis was performed using MaxQuant 1.2.2.5 (Cox and Mann, 2008). Variable modification was set to oxidation of methionine, fixed modification was set to carbamidomethylation of cysteine, and dimethyl labelling was selected as quantification method. Completeness of labelling was judged by searching for unlabeled peptides. MS/MS spectra were searched against the UniProt *S. coelicolor* reference proteome set (organism 100226, excluding SCP1 plasmid proteins, version 2012_06) with a false discovery rate of 1% for both proteins and peptides, and an additional second peptide search was performed (Cox *et al*., 2011). Quantification was performed as described (Cox and Mann, 2008). In short, a median protein expression ratio was determined using normalized expression ratios of positively identified peptides and of low-scoring versions of peptides already positively identified in a separate MS/MS event. No median ratio was determined when less than three peptide ratios were available. All samples grown in the presence of mannitol were analysed in one MaxQuant run, and all samples grown in the presence of fructose in a separate run. Complete MaxQuant output tables have been submitted to the Dryad digital repository (http://dx.doi.org/10.5061/dryad.62j0q).

Acknowledgements

The work was supported by an ECHO grant from the Netherlands Society for Scientific Research (NWO) to GPvW and by a VENI grant from the Dutch Technology Foundation (STW) to JG.

References

Angell, S., Schwarz, E., and Bibb, M.J. (1992) The glucose kinase gene of *Streptomyces coelicolor* A3(2): its nucleotide sequence, transcriptional analysis and role in glucose repression. *Mol Microbiol* **6:** 2833–2844.

Angell, S., Lewis, C.G., Buttner, M.J., and Bibb, M.J. (1994) Glucose repression in *Streptomyces coelicolor* A3(2): a likely regulatory role for glucose kinase. *Mol Gen Genet* **244:** 135–143.

Barends, S., Zehl, M., Bialek, S., de Waal, E., Traag, B.A., Willemse, J., *et al*. (2010) Transfer-messenger RNA controls the translation of cell-cycle and stress proteins in *Streptomyces*. *EMBO Rep* **11:** 119–125.

Bentley, S.D., Chater, K.F., Cerdeno-Tarraga, A.M., Challis, G.L., Thomson, N.R., James, K.D., *et al*. (2002) Complete genome sequence of the model actinomycete *Streptomyces coelicolor* A3(2). *Nature* **417:** 141–147.

Bibb, M.J., Molle, V., and Buttner, M.J. (2000) sigma(BldN), an extracytoplasmic function RNA polymerase sigma factor required for aerial mycelium formation in *Streptomyces coelicolor* A3(2). *J Bacteriol* **182:** 4606–4616.

Boersema, P.J., Raijmakers, R., Lemeer, S., Mohammed, S., and Heck, A.J. (2009) Multiplex peptide stable isotope dimethyl labeling for quantitative proteomics. *Nat Protoc* **4:** 484–494.

Brückner, R., and Titgemeyer, F. (2002) Carbon catabolite repression in bacteria: choice of the carbon source and autoregulatory limitation of sugar utilization. *FEMS Microbiol Lett* **209:** 141–148.

Challis, G.L., and Hopwood, D.A. (2003) Synergy and contingency as driving forces for the evolution of multiple secondary metabolite production by *Streptomyces* species. *Proc Natl Acad Sci USA* **100:** 14555–14561.

Chater, K.F. (2001) Regulation of sporulation in *Streptomyces coelicolor* A3(2): a checkpoint multiplex? *Curr Opin Microbiol* **4:** 667–673.

Chater, K.F., Biro, S., Lee, K.J., Palmer, T., and Schrempf, H. (2010) The complex extracellular biology of *Streptomyces*. *FEMS Microbiol Rev* **34:** 171–198.

Cox, J., and Mann, M. (2008) MaxQuant enables high peptide identification rates, individualized p.p.b.-range mass accuracies and proteome-wide protein quantification. *Nat Biotechnol* **26:** 1367–1372.

Cox, J., Neuhauser, N., Michalski, A., Scheltema, R.A., Olsen, J.V., and Mann, M. (2011) Andromeda: a peptide search engine integrated into the MaxQuant environment. *J Proteome Res* **10:** 1794–1805.

Davidson, A.L., Dassa, E., Orelle, C., and Chen, J. (2008) Structure, function, and evolution of bacterial ATP-binding cassette systems. *Microbiol Mol Biol Rev* **72:** 317–364, table of contents.

Demain, A.L. (1999) Pharmaceutically active secondary metabolites of microorganisms. *Appl Microbiol Biotechnol* **52:** 455–463.

Feitelson, J.S., Malpartida, F., and Hopwood, D.A. (1985) Genetic and biochemical characterization of the *red* gene cluster of *Streptomyces coelicolor* A3(2). *J Gen Microbiol* **131:** 2431–2441.

Flärdh, K., and Buttner, M.J. (2009) *Streptomyces* morphogenetics: dissecting differentiation in a filamentous bacterium. *Nat Rev Microbiol* **7:** 36–49.

Gorke, B., and Stulke, J. (2008) Carbon catabolite repression in bacteria: many ways to make the most out of nutrients. *Nat Rev Microbiol* **6:** 613–624.

Gramajo, H.C., Takano, E., and Bibb, M.J. (1993) Stationary-phase production of the antibiotic actinorhodin in *Streptomyces coelicolor* A3(2) is transcriptionally regulated. *Mol Microbiol* **7:** 837–845.

Guzman, S., Ramos, I., Moreno, E., Ruiz, B., Rodriguez-Sanoja, R., Escalante, L., *et al*. (2005) Sugar uptake and sensitivity to carbon catabolite regulation in *Streptomyces peucetius* var. *caesius*. *Appl Microbiol Biotechnol* **69:** 200–206.

den Hengst, C.D., Tran, N.T., Bibb, M.J., Chandra, G., Leskiw, B.K., and Buttner, M.J. (2010) Genes essential for morphological development and antibiotic production in *Streptomyces coelicolor* are targets of BldD during vegetative growth. *Mol Microbiol* **78:** 361–379.

Hopwood, D.A. (2007) *Streptomyces in Nature and Medicine: the Antibiotic Makers*. New York: Oxford University Press.

Ingram, C., and Westpheling, J. (1995) The glucose kinase gene of *Streptomyces coelicolor* is not required for glucose repression of the *chi63* promoter. *J Bacteriol* **177:** 3587–3588.

Jakimowicz, D., and van Wezel, G.P. (2012) Cell division and DNA segregation in *Streptomyces*: how to build a septum in the middle of nowhere? *Mol Microbiol* **85:** 393–404.

Keijser, B.J., Noens, E.E., Kraal, B., Koerten, H.K., and van Wezel, G.P. (2003) The *Streptomyces coelicolor ssgB* gene is required for early stages of sporulation. *FEMS Microbiol Lett* **225:** 59–67.

Kieser, T., Bibb, M.J., Buttner, M.J., Chater, K.F., and Hopwood, D.A. (2000) *Practical* Streptomyces *Genetics*. Norwich: The John Innes Foundation.

Kwakman, J.H., and Postma, P.W. (1994) Glucose kinase has a regulatory role in carbon catabolite repression in *Streptomyces coelicolor*. *J Bacteriol* **176:** 2694–2698.

Liu, H., and Reynolds, K.A. (2001) Precursor supply for polyketide biosynthesis: the role of crotonyl-CoA reductase. *Metab Eng* **3:** 40–48.

Lunin, V.V., Li, Y., Schrag, J.D., Iannuzzi, P., Cygler, M., and Matte, A. (2004) Crystal structures of *Escherichia coli* ATP-dependent glucokinase and its complex with glucose. *J Bacteriol* **186:** 6915–6927.

Mahr, K., van Wezel, G.P., Svensson, C., Krengel, U., Bibb, M.J., and Titgemeyer, F. (2000) Glucose kinase of *Streptomyces coelicolor* A3(2): large-scale purification and biochemical analysis. *Antonie Van Leeuwenhoek* **78:** 253–261.

Manteca, A., Jung, H.R., Schwammle, V., Jensen, O.N., and Sanchez, J. (2010a) Quantitative proteome analysis of *Streptomyces coelicolor* nonsporulating liquid cultures demonstrates a complex differentiation process comparable to that occurring in sporulating solid cultures. *J Proteome Res* **9:** 4801–4811.

Manteca, A., Sanchez, J., Jung, H.R., Schwammle, V., and Jensen, O.N. (2010b) Quantitative proteomics analysis of *Streptomyces coelicolor* development demonstrates that onset of secondary metabolism coincides with hypha differentiation. *Mol Cell Proteomics* **9:** 1423–1436.

Marsden, A.F., Wilkinson, B., Cortes, J., Dunster, N.J., Staunton, J., and Leadlay, P.F. (1998) Engineering broader specificity into an antibiotic-producing polyketide synthase. *Science* **279:** 199–202.

Martinez, A., Kolvek, S.J., Hopke, J., Yip, C.L., and Osburne, M.S. (2005) Environmental DNA fragment conferring early and increased sporulation and antibiotic production in *Streptomyces* species. *Appl Environ Microbiol* **71:** 1638–1641.

Milenbachs, A.A., Brown, D.P., Moors, M., and Youngman, P. (1997) Carbon-source regulation of virulence gene expres-

sion in *Listeria monocytogenes*. *Mol Microbiol* **23:** 1075–1085.
Miyazono, K., Tabei, N., Morita, S., Ohnishi, Y., Horinouchi, S., and Tanokura, M. (2012) Substrate recognition mechanism and substrate-dependent conformational changes of an ROK family glucokinase from *Streptomyces griseus*. *J Bacteriol* **194:** 607–616.
Nothaft, H., Rigali, S., Boomsma, B., Swiatek, M., McDowall, K.J., van Wezel, G.P., and Titgemeyer, F. (2010) The permease gene *nagE2* is the key to N-acetylglucosamine sensing and utilization in *Streptomyces coelicolor* and is subject to multi-level control. *Mol Microbiol* **75:** 1133–1144.
Olsen, J.V., de Godoy, L.M., Li, G., Macek, B., Mortensen, P., Pesch, R., *et al*. (2005) Parts per million mass accuracy on an Orbitrap mass spectrometer via lock mass injection into a C-trap. *Mol Cell Proteomics* **4:** 2010–2021.
Pao, S.S., Paulsen, I.T., and Saier, M.H., Jr (1998) Major facilitator superfamily. *Microbiol Mol Biol Rev* **62:** 1–34.
Park, S.S., Yang, Y.H., Song, E., Kim, E.J., Kim, W.S., Sohng, J.K., *et al*. (2009) Mass spectrometric screening of transcriptional regulators involved in antibiotic biosynthesis in *Streptomyces coelicolor* A3(2). *J Ind Microbiol Biotechnol* **36:** 1073–1083.
Patton, S.M., Cropp, T.A., and Reynolds, K.A. (2000) A novel delta(3),delta(2)-enoyl-CoA isomerase involved in the biosynthesis of the cyclohexanecarboxylic acid-derived moiety of the polyketide ansatrienin A. *Biochemistry* **39:** 7595–7604.
Piette, A., Derouaux, A., Gerkens, P., Noens, E.E., Mazzucchelli, G., Vion, S., *et al*. (2005) From dormant to germinating spores of *Streptomyces coelicolor* A3(2): new perspectives from the *crp* null mutant. *J Proteome Res* **4:** 1699–1708.
Pope, M.K., Green, B.D., and Westpheling, J. (1996) The *bld* mutants of *Streptomyces coelicolor* are defective in the regulation of carbon utilization, morphogenesis and cell–cell signalling. *Mol Microbiol* **19:** 747–756.
Pope, M.K., Green, B., and Westpheling, J. (1998) The *bldB* gene encodes a small protein required for morphogenesis, antibiotic production, and catabolite control in *Streptomyces coelicolor*. *J Bacteriol* **180:** 1556–1562.
Rappsilber, J., Mann, M., and Ishihama, Y. (2007) Protocol for micro-purification, enrichment, pre-fractionation and storage of peptides for proteomics using StageTips. *Nat Protoc* **2:** 1896–1906.
Rigali, S., Titgemeyer, F., Barends, S., Mulder, S., Thomae, A.W., Hopwood, D.A., and van Wezel, G.P. (2008) Feast or famine: the global regulator DasR links nutrient stress to antibiotic production by *Streptomyces*. *EMBO Rep* **9:** 670–675.
Rodriguez, E., Banchio, C., Diacovich, L., Bibb, M.J., and Gramajo, H. (2001) Role of an essential acyl coenzyme A carboxylase in the primary and secondary metabolism of *Streptomyces coelicolor* A3(2). *Appl Environ Microbiol* **67:** 4166–4176.
Rodriguez, E., Navone, L., Casati, P., and Gramajo, H. (2012) Impact of malic enzymes on antibiotic and triacylglycerol production in *Streptomyces coelicolor*. *Appl Environ Microbiol* **78:** 4571–4579.
Sanchez, S., Chavez, A., Forero, A., Garcia-Huante, Y., Romero, A., Sanchez, M., *et al*. (2010) Carbon source regulation of antibiotic production. *J Antibiot (Tokyo)* **63:** 442–459.
Sauer, U., and Eikmanns, B.J. (2005) The PEP-pyruvate-oxaloacetate node as the switch point for carbon flux distribution in bacteria. *FEMS Microbiol Rev* **29:** 765–794.
Schlösser, A., Kampers, T., and Schrempf, H. (1997) The *Streptomyces* ATP-binding component MsiK assists in cellobiose and maltose transport. *J Bacteriol* **179:** 2092–2095.
Shelburne, S.A., 3rd, Keith, D., Horstmann, N., Sumby, P., Davenport, M.T., Graviss, E.A., *et al*. (2008) A direct link between carbohydrate utilization and virulence in the major human pathogen group A *Streptococcus*. *Proc Natl Acad Sci USA* **105:** 1698–1703.
Swiatek, M.A., Tenconi, E., Rigali, S., and van Wezel, G. (2012a) Functional analysis of the N-acetylglucosamine metabolic genes of *Streptomyces coelicolor* and role in the control of development and antibiotic production. *J Bacteriol* **194:** 1136–1144.
Swiatek, M.A., Urem, M., Tenconi, E., Rigali, S., and van Wezel, G.P. (2012b) Engineering of N-acetylglucosamine metabolism for improved antibiotic production in *Streptomyces coelicolor* A3(2) and an unsuspected role of NagA in glucosamine metabolism. *Bioengineered* **3:** 280–285. doi:10.4161/bioe.21371
Takano, E., Chakraburtty, R., Nihira, T., Yamada, Y., and Bibb, M.J. (2001) A complex role for the gamma-butyrolactone SCB1 in regulating antibiotic production in *Streptomyces coelicolor* A3(2). *Mol Microbiol* **41:** 1015–1028.
Takano, E., Kinoshita, H., Mersinias, V., Bucca, G., Hotchkiss, G., Nihira, T., *et al*. (2005) A bacterial hormone (the SCB1) directly controls the expression of a pathway-specific regulatory gene in the cryptic type I polyketide biosynthetic gene cluster of *Streptomyces coelicolor*. *Mol Microbiol* **56:** 465–479.
Thorpe, C., and Kim, J.J. (1995) Structure and mechanism of action of the acyl-CoA dehydrogenases. *FASEB J* **9:** 718–725.
Titgemeyer, F., Reizer, J., Reizer, A., and Saier, M.H., Jr (1994) Evolutionary relationships between sugar kinases and transcriptional repressors in bacteria. *Microbiology* **140:** 2349–2354.
Titgemeyer, F., Amon, J., Parche, S., Mahfoud, M., Bail, J., Schlicht, M., *et al*. (2007) A genomic view of sugar transport in *Mycobacterium smegmatis* and *Mycobacterium tuberculosis*. *J Bacteriol* **189:** 5903–5915.
Tong, L. (2005) Acetyl-coenzyme A carboxylase: crucial metabolic enzyme and attractive target for drug discovery. *Cell Mol Life Sci* **62:** 1784–1803.
Wang, W., Shu, D., Chen, L., Jiang, W., and Lu, Y. (2009) Cross-talk between an orphan response regulator and a noncognate histidine kinase in *Streptomyces coelicolor*. *FEMS Microbiol Lett* **294:** 150–156.
Wessel, D., and Flugge, U.I. (1984) A method for the quantitative recovery of protein in dilute solution in the presence of detergents and lipids. *Anal Biochem* **138:** 141–143.
van Wezel, G., Konig, M., Mahr, K., Nothaft, H., Thomae, A.W., Bibb, M., and Titgemeyer, F. (2007) A new piece of an old jigsaw: glucose kinase is activated posttranslationally in a glucose transport-dependent manner in *Streptomyces coelicolor* A3(2). *J Mol Microbiol Biotechnol* **12:** 67–74.

van Wezel, G.P., and McDowall, K.J. (2011) The regulation of the secondary metabolism of *Streptomyces*: new links and experimental advances. *Nat Prod Rep* **28:** 1311–1333.

van Wezel, G.P., White, J., Bibb, M.J., and Postma, P.W. (1997a) The *malEFG* gene cluster of *Streptomyces coelicolor* A3(2): characterization, disruption and transcriptional analysis. *Mol Gen Genet* **254:** 604–608.

van Wezel, G.P., White, J., Young, P., Postma, P.W., and Bibb, M.J. (1997b) Substrate induction and glucose repression of maltose utilization by *Streptomyces coelicolor* A3(2) is controlled by *malR*, a member of the *lacI-galR* family of regulatory genes. *Mol Microbiol* **23:** 537–549.

van Wezel, G.P., Mahr, K., Konig, M., Traag, B.A., Pimentel-Schmitt, E.F., Willimek, A., and Titgemeyer, F. (2005) GlcP constitutes the major glucose uptake system of *Streptomyces coelicolor* A3(2). *Mol Microbiol* **55:** 624–636.

van Wezel, G.P., Krabben, P., Traag, B.A., Keijser, B.J., Kerste, R., Vijgenboom, E., *et al*. (2006) Unlocking *Streptomyces* spp. for use as sustainable industrial production platforms by morphological engineering. *Appl Environ Microbiol* **72:** 5283–5288.

Willemse, J., Borst, J.W., de Waal, E., Bisseling, T., and van Wezel, G.P. (2011) Positive control of cell division: FtsZ is recruited by SsgB during sporulation of *Streptomyces*. *Genes Dev* **25:** 89–99.

Yang, Y.H., Song, E., Kim, J.N., Lee, B.R., Kim, E.J., Park, S.H., *et al*. (2012) Characterization of a new ScbR-like gamma-butyrolactone binding regulator (SlbR) in *Streptomyces coelicolor*. *Appl Microbiol Biotechnol* **96:** 113–121.

Supporting information

Additional supporting information may be found in the online version of this article.